00

Optical spectra of a photonic crystal structure with graphene layers

© S.V. Eliseeva, D.I. Sementsov

Ulyanovsk State University,
432017 Ulyanovsk, Russia

e-mail: eliseeva-sv@yandex.ru

The transformation of the graphene-containing optical spectra photonic-crystal structure with a change in the chemical potential (μ) of graphene is studied. In the period of the structure, one layer is a graphene-containing periodic medium $(SiO_2/Gr)^n$, and the second layer is assumed to be made of pure silicon. In the case of unexcited graphene ($\mu = 0$), the absorption in the structure exceeds the reflection and transmission for frequencies outside the photonic band gaps. Within these zones, most of the incident radiation is reflected, and there is no transmission at all. As μ increases outside the band gaps, the absorption decreases in the low-frequency region, and the transmission increases the stronger, the greater μ. In a structure with an inversion defect inside the band gaps, either suppression or significant rearrangement of the defect mode takes place.

Keywords: graphene, effective medium, photonic crystal structure, transfer matrices, reflection, transmission and absorption spectra, photonic band gap, defect mode.

DOI: 10.21883/0000000000

Introduction

Over the past decade, the amazing optical properties of graphene have become the subject of widespread research and discussion [1–6]. In particular, one of the fundamental properties of graphene was revealed - even one of its sheets (i.e., a monoatomic layer) can absorb a significant part of the incident radiation, namely $A \approx \pi\alpha \approx 0.023$, where $\alpha = e^2/c\hbar$ — fine structure constant [7,8]. This is primarily due to the Dirac spectrum and zero electron mass of graphene, which lead to high electron mobility, high conductivity and a significant difference in its optical properties from the properties of traditional materials.

Let us note that despite special attention to graphene as the supposed ground element of the electronics of the future, at present silicon structures still play a key role. Therefore, the development of „graphene“ electronics at this interval is not associated with the replacement of silicon elements with graphene ones, but with the gradual integration of graphene with structures based on silicon and its compounds. The combination of graphene and a semiconductor substrate with the appropriate thickness and dielectric constant (DC) allows to effectively control the optical spectrum of such a structure by changing the chemical potential of graphene by an electric field [9–13].

This paper is devoted to the study of the spectral characteristics of a finite photonic crystal structure (PCS), consisting of m periods. The first layer of the period is a finite planar layered structure of a repeating n fold system of layers — „silicon dioxide/graphene“. The second layer in the PCS period is assumed to be made of pure silicon. The influence of the energy state of graphene, determined by its chemical potential, on the optical spectra of reflection, transmission and absorption of the PCS is studied.

Constitutive parameters

Consider a finite PCS $[(SiO_2/Gr)^n]^m$ with the number of periods $m = 20$. The period of the structure includes two layers, optically isotropic in their plane, with thicknesses L_1 and L_2. The material of the first layer is a structure consisting of $N = 10$ layers of silicon dioxide and graphene, $(SiO_2/Gr)^n$. The second layer in the PCS period is pure silicon (Fig. 1). Let us assume that the DC of the coating medium and the substrate is $\varepsilon_a = \varepsilon_b = 1$. The permeabilities of all materials are equal to unity. Such a structure has a preferred direction normal to the interface between the layers, which determines the uniaxial anisotropy of its properties.

Many of the electrodynamic properties of graphene are related to its surface conductivity, which, in turn, is determined by the chemical potential μ. In undoped (pure) graphene, the chemical potential is at the Dirac point, and applying a voltage of different polarity (i.e., doping graphene with electrons or holes) allows it to be shifted to the conduction band or valence band. The chemical potential

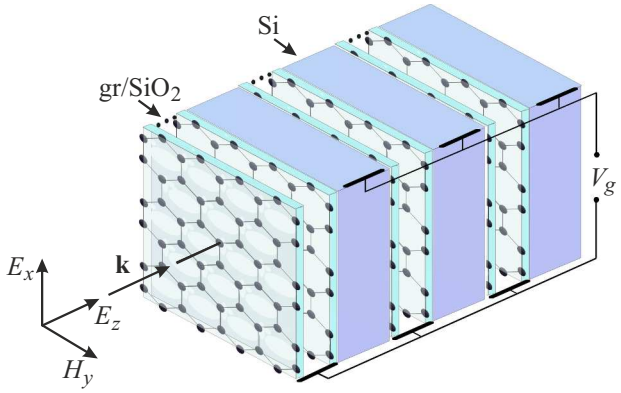

Figure 1. Geometry of the problem.

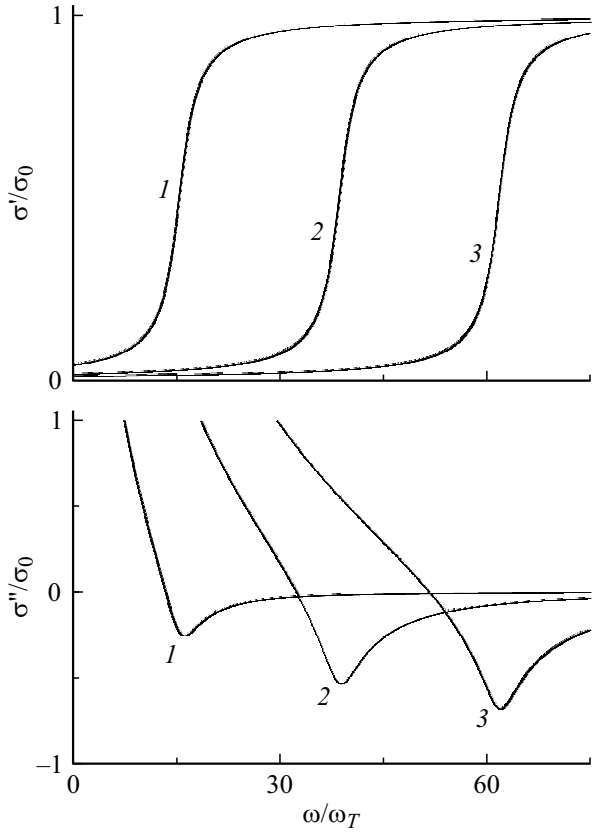

Figure 2. Frequency dependence of the real and imaginary parts of the normalized conductivity of graphene and the DC of the effective medium SiO_2/Gr at $\mu = (0.2,\ 0.5,\ 0.8)$ eV (curves *1, 2* and *3*, respectively).

can be controlled by an external electric field normal to the surface of the graphene sheet. The dependence of the chemical potential on the external field strength E_0 is determined by the expression [19,20]

$$E_0 = \frac{e}{\pi\hbar^2 v_F^2 \varepsilon_b} \int_0^\infty \varepsilon(f(\varepsilon) - f(\varepsilon + 2\mu))d\varepsilon, \qquad (1)$$

where $f(\varepsilon)$ — Fermi distribution – Dirac, ε — electron energy, $\hbar$ — Planck's constant, $v_F = 3\gamma_0/2\hbar$ — Fermi velocity, where $\gamma_0 = 2.7$ eV, b — distance between neighboring atoms in the graphene structure, ε_b — DC substrate. Figure 2 shows the dependence of the chemical potential of graphene on the strength of the external electric field, obtained for the values of $b = 0.2$ nm and the substrate DC ε_b = 1,5.07, 10.9 (for vacuum, SiO_2 and Si, respectively — curves *1–3*). It can be seen that with increasing potential applied to the graphene layer, the value μ increases the faster, the greater the substrate DC.

Thus, by applying a voltage between the graphene sheet and the substrate, it is possible to change the chemical potential and thereby its surface conductivity. The dependence of the real and imaginary parts of the complex surface conductivity of doped graphene on frequency and chemical

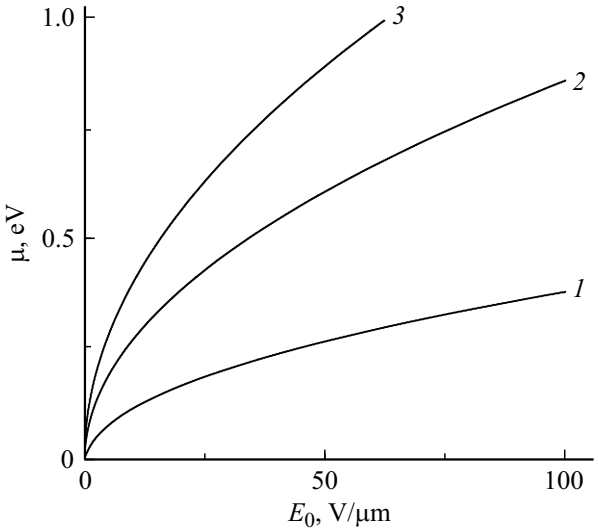

Figure 3. Dependence of the chemical potential of graphene on the external electric field strength at $\varepsilon_b = 1,\ 5.07,\ 10.9$ (curves *1, 2, 3*, respectively).

potential is determined by the expressions [16–18]

$$\frac{\sigma'}{\sigma_0} = \frac{1}{2} + \frac{1}{\pi}\,\mathrm{arctg}\left(\frac{\hbar\omega - 2\mu}{2k_b T}\right),$$

$$\frac{\sigma''}{\sigma_0} = \frac{1}{2\pi}\left[\frac{16k_B T}{\hbar\omega}\ln\left(2\cosh\left(\frac{\mu}{2k_B T}\right)\right) - \ln\left(\frac{(\hbar\omega + 2\mu)^2}{(\hbar\omega - 2\mu)^2 + (2k_B T)^2}\right)\right], \qquad (2)$$

where $\sigma_0^2/4\hbar$, e — electron charge, k_B — Boltzmann constant, T — temperature.

Figure 3, *a, b* shows the frequency dependences of the real and imaginary parts of the conductivity of graphene for chemical potential values $\mu = (0.2,\ 0.5,\ 0.8)$ eV (curves *1–3*, respectively), which can be changed experimentally using an external electric field. Here and below, the numerical analysis is carried out for the operating temperature $T = 300$ K. The presented dependencies use the frequency normalized to the value ($\omega_T = k_B T/\hbar = 3.93 \cdot 10^{13}\ \mathrm{s}^{-1}$) (constant at $T = \mathrm{const}$). It can be seen that in the frequency range under consideration, the real part of the conductivity is positive (which corresponds to the absorption mode in graphene); with increasing chemical potential, the growth area σ' shifts to the area of higher frequencies. The same shift is experienced by the imaginary part of the conductivity, which takes negative values in a fairly wide frequency range, reaching its lowest value at $\omega = \omega_\mu = 2\mu/\hbar$.

Main equations

Let us assume that a linearly polarized wave propagates in the structure along the axis of symmetry, which is perpendicular to the interfaces between the layers (Fig. 1). The first

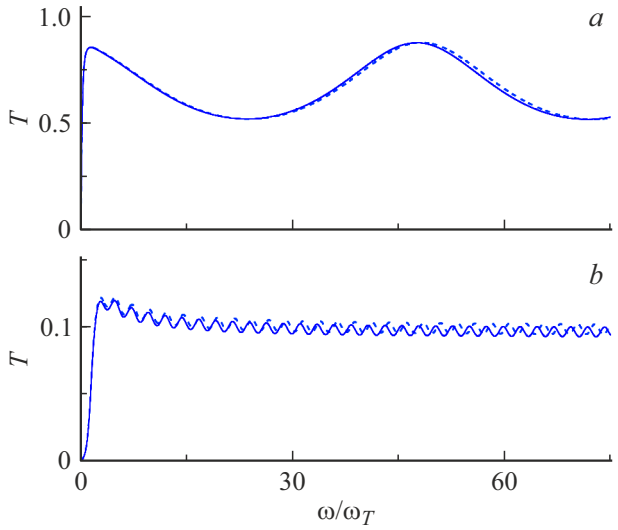

Figure 4. Frequency dependence of the transmission factor for one period (SiO_2/Gr) with thickness $L_{SiO_2} + L_{Gr} = 0.22\,\mu$m and a structure of twenty similar periods (a, b) for the chemical potential $\mu = 0$, (solid line —matrix method, dashed — effective medium method).

layer in the PCS period is a flat-layered medium $(SiO_2/Gr)^n$, which consists of alternating layers of silicon oxide and graphene with DC $\varepsilon_{SiO_2} = 5.07$, $\varepsilon_{Gr} = 1 + i4\pi\sigma/\omega L_{Gr}$ and thicknesses $L_{SiO_2} = 0.022\,\mu$m, $L_{Gr} = 0.335$ nm. The amplitude transmission and reflection factors for the PCS are expressed through the matrix elements of the transfer matrix of the entire $\hat{G}$ structure, which connects the amplitudes of the incident and emerging waves:

$$t = \frac{2}{G_{11} + G_{12} + G_{21} + G_{22}},$$

$$r = \frac{G_{11} + G_{12} - G_{21} - G_{22}}{G_{11} + G_{12} + G_{21} + G_{22}}. \qquad (3)$$

For the structure under consideration $[(SiO_2/Gr)^n]^m$ the transfer matrix has the form $G = [(M_1M_2)^nM_3]^m$, where the transfer matrices of the corresponding layers [21]

$$M_j = \begin{pmatrix} \cos(k_jL_j) & -i\sqrt{\varepsilon_j}\sin(k_jL_j) \\ -(i/\sqrt{\varepsilon_j})\sin(k_jL_j) & \cos(k_jL_j) \end{pmatrix} \qquad (4)$$

Here $k_j = k_0\sqrt{\varepsilon_j}$ — propagation constant in the corresponding layer, $k_0 = \omega/c$, ω and c — frequency and wave speed in vacuum, for graphene layers $k_{Gr} = k_0\sqrt{\varepsilon_{Gr}}$. The $M_{1,2}$ matrices correspond to the corresponding layer of the structure period $(SiO_2/Gr)^n$, and the M_1 matrix corresponds to the silicon layers. The energy reflectances and transmission in this case have the form $R = |r|^2$, $T = |t|^2$. When taking into account absorption in the layers, the absorption factor (the fraction of energy absorbed by the PCS) is defined by the expression $A = 1 - R - T$.

In many papers, the optical properties of a graphene-containing planar-layered structure are described within the

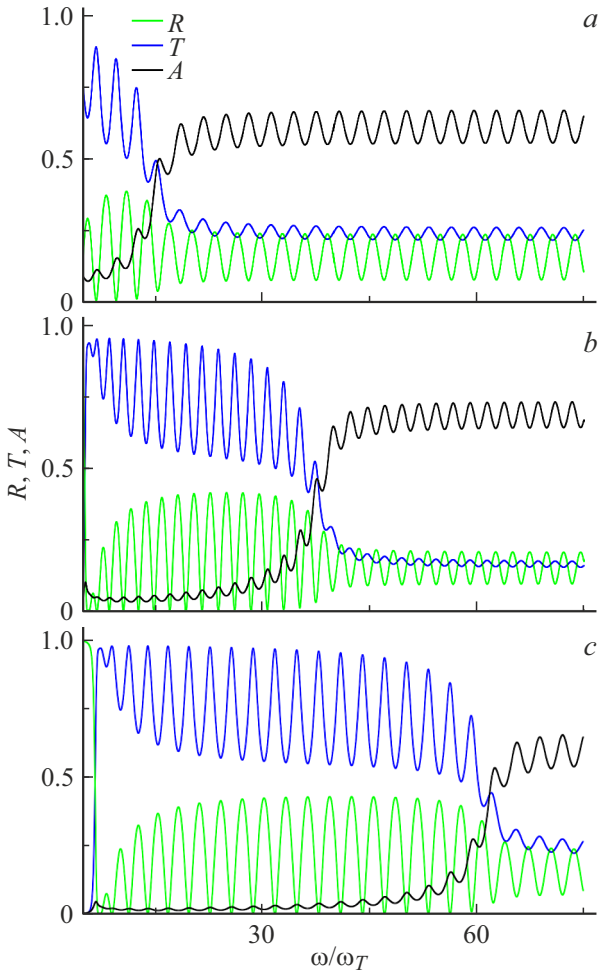

Figure 5. Frequency dependence of the reflectance, transmission and absorption factors (R, T and A) for the effective medium layer $(SiO_2/Gr)^{20}$, $L = 20L_1 = 4.4\,\mu$m, $\mu = (0.2, 0.5, 0.8)$ eV (a, b and c respectively).

framework of the effective medium model (fine-layered approximation). In this approximation (L_{SiO_2}), $T = |t|^2$ effective DC

$$\varepsilon_{ef} = \frac{\varepsilon_{SiO_2}L_{SiO_2} + \varepsilon_{Gr}L_{Gr}}{L_{SiO_2} + L_{Gr}} = \frac{1}{\theta + 1}\left(\varepsilon_{SiO_2} - \frac{4\pi\sigma''}{\omega L_{SiO_2}} + i\frac{4\pi\sigma'}{\omega L_{SiO_2}}\right), \qquad (5)$$

where the parameter $\theta = L_{Gr}/L_{SiO_2}$. The DC of graphene ε_{Gr} is related to its complex surface conductivity by the relation $\varepsilon_{Gr} = 1 + i4\pi(\sigma' + i\sigma'')/\omega L_{Gr}$. In real structures the parameter $\theta \ll 1$, and expression (5) coincides with ε_{ef} obtained in the papers [15,16]:

$$\varepsilon_{ef} = \varepsilon_{SiO_2} - \frac{4\pi\sigma''}{\omega L_{SiO_2}} + i\frac{4\pi\sigma'}{\omega L_{SiO_2}}. \qquad (6)$$

Figure 4 shows the frequency dependence of the transmission coefficient for one period (SiO_2/Gr) (graphene

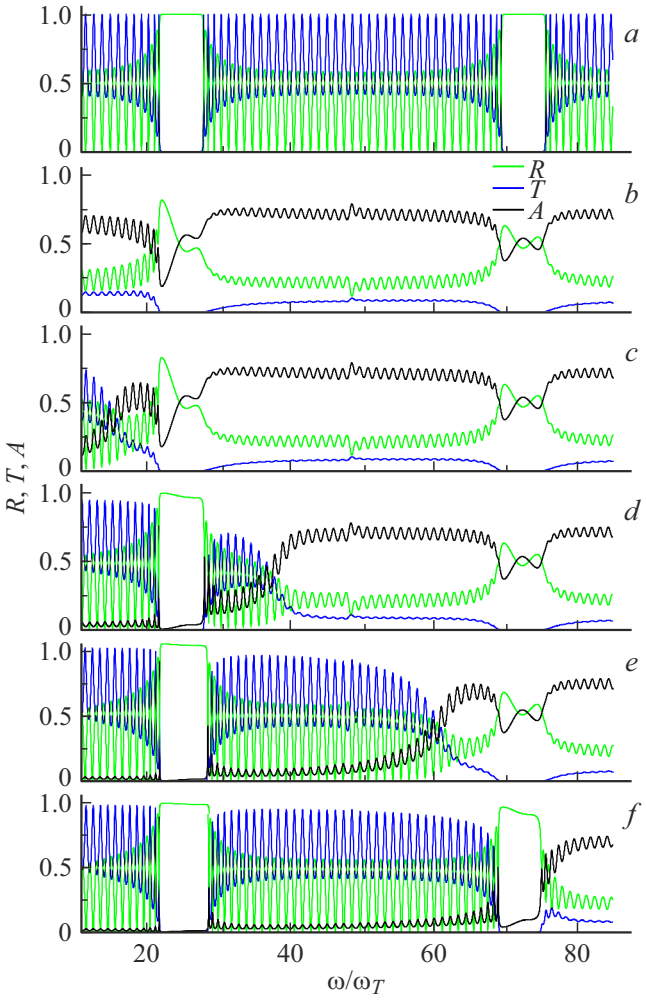

Figure 6. Frequency dependence of energy coefficients R, T and A for structures $(SiO_2/Si)^{20}$ (a) and at $\mu = (0,\ 0.2,\ 0.5,\ 0.8,\ 1.0)$ eV $(b, c, d, e, f$ respectively), $L_1 = \lambda_0/4n_{ef} = 0.22\,\mu$m, $(L_2 = \lambda_0/4n_{SiO_2} = 0.15\,\mu$m).

on a silicon dioxide substrate) with a thickness of $L_{SiO_2} + L_{Gr} = 0.22\,\mu$m and a structure of twenty of the same periods with a total thickness of $4.4\,\mu$m (a, b). The calculation used the value of the chemical potential of graphene $\mu = 0$. The dependences were obtained by two methods: in the approximation of a fine-layered medium using the effective DC ε_{ef} (dashed line) and based on the matrix approach (solid line) using transfer matrices (M_1M_2) and $(M_1M_2)^{20}$ for one and twenty periods. It can be seen that both approaches for the selected period of the structure give similar results.

Next, to model the optical spectra of the structure under study, we use a matrix approach.

Numerical analysis

The figures below show the frequency dependences of the energy reflectances, transmission and absorption (green, blue and black curves), obtained on the basis of numerical analysis for PCS implemented on the basis of a controlled effective graphene medium. Figure 5 shows the frequency dependence of the factors R, T and A (green, blue, black lines) for the structure $(SiO_2/Gr)^{20}$ with the value of its period $L_{SiO_2} + L_{Gr} = 0.22\,\mu$m and the values of the chemical potential $\mu = (0.2,\ 0.5,\ 0.8)$ eV $(a, b, c$ respectively). For the graphene-containing structure under study, absorption is present at all frequencies. At low frequencies, transmission predominates over reflection and absorption; with increasing frequency, transmittance decreases, and reflection in a wide frequency range remains almost at the same level. In this case, the quantities R, T and A are oscillating functions of frequency, which is associated with the manifestation of interference at a given layer thickness. The presence of graphene in the structure leads to a significant restructuring of the spectrum, in particular to a high fraction of absorption, which depends on the value of the chemical potential of graphene and increases with increasing frequency. At $\mu = 0.2$ eV the structure absorbs a significant part of the radiation in a wide frequency range, while with $\mu = 0.8$ eV the structure begins to absorb only at sufficiently high frequencies $(\omega \geq 50\omega_T)$. Let us note that for a structure without graphene $(SiO_2)^{20}$ there is no absorption, since it is accepted that in the frequency range under consideration ε_{SiO_2} — an actual value. The transmittance spectrum contains well-resolved narrow regions of almost complete transparency, lying in different parts of the spectrum for different chemical potential values.

Figure 6 shows the frequency dependence of the factors R, T and A for structures (SiO_2/Gr^{20}) (a) and $((SiO_2/Gr)^{10}/Si)^{20}$ with quarter-wave layer thickness $L_1 = \lambda_0/4n_{SiO_2} = 0.22\,\mu$m, $L_2 = \lambda_0/4n_{Si} = 0.15\,\mu$m ($\lambda_0$ at $\omega_0/\omega_T = 24$) and chemical potential values $\mu = (0,\ 0.2,\ 0.5,\ 0.8,\ 1.0)$ eV $(b-f$, respectively). It can be seen that in the spectrum of PCS that does not contain graphene, there is an alternation of well-resolved transmittance and non-transmittance bands, as well as the absence of absorption. In this case, in the entire frequency range, with the exception of photonic band gaps (PBG), there is an alternation of narrow areas with high values (close to unity) of the factors R and T

For a periodic graphene structure, a significant influence on the spectra of the values R, T and A of the energy state of graphene, determined by the value of the chemical potential, is visible. In case of unexcited graphene $(\mu = 0)$, absorption in the structure exceeds reflection and transmission for frequencies lying outside the BG, while inside these zones most of the incident radiation is reflected and there is no transmission at all. With an increase in the chemical potential outside the PBG, the absorption decreases in the low-frequency region, and the transmission increases the more strongly, the greater the μ. Inside the first BG, with increasing μ, absorption and transmission are suppressed, and the PCS at the corresponding frequencies can be used as an effective reflector. In the second PBG,

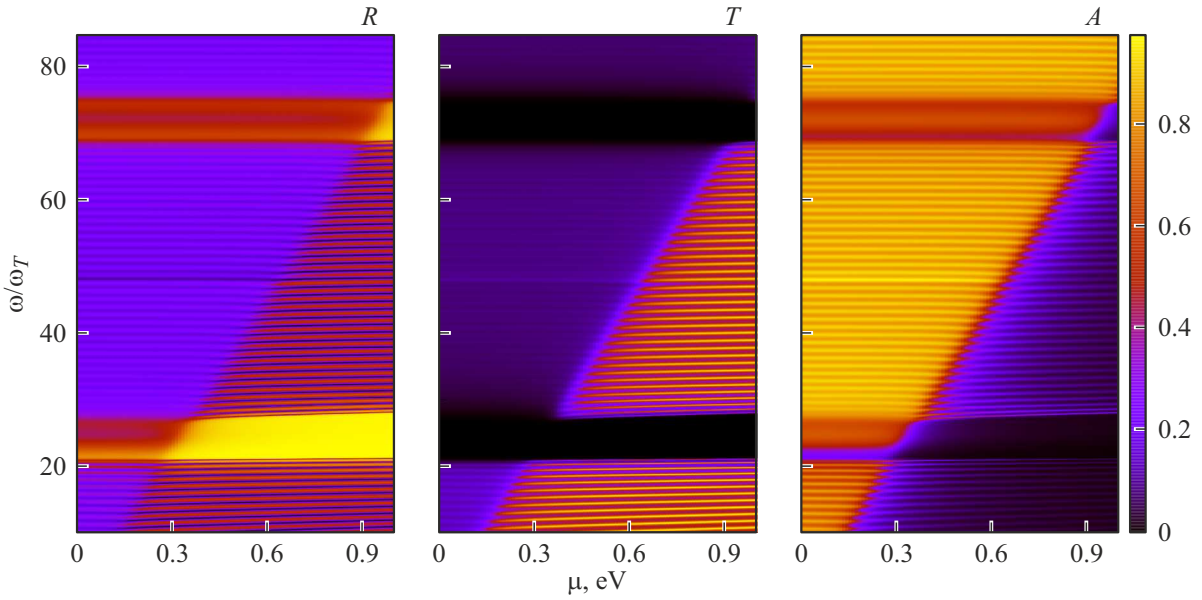

Figure 7. Dependence of the energy factors R, T and A for the structure $((SiO_2/Gr)^{10}/Si)^{20}$ on frequency and chemical potential, $L_1 = 0.22\,\mu$m, $L_2 = 0.15\,\mu$m.

the dependency profiles $R(\omega)$ and $A(\omega)$ practically do not change with increasing μ. The transmission outside the PBG increases with increasing chemical potential, and the absorption spectrum contains well-resolved narrow areas of almost complete transparency. There is no passage within each of the PBG for all chemical potential values.

Figure 7 shows a tone diagram (color map) of the reflectance, absorption and transmission coefficients for PCS $((SiO_2/Gr)^{10}/Si)^{20}$ with quarter-wave layer thickness (for $\lambda_0 = 2\,\mu$m, $\omega/\omega_r = 24$), characterizing the dependence of energy coefficients on frequency and chemical potential . It can be seen that the diagrams in the corresponding frequency intervals contain both areas of maximum reflection and areas of significant absorption. Thus, the presence of a layer $(SiO_2/Gr)^{10}$ in the PCS period allows, by controlling the chemical potential of graphene, to rearrange the photon spectra, changing the transmission and absorption of radiation incident on the structure, which allows the use of this structure as an effective reflector and absorber of radiation.

An important type of PCS are structures containing a defect that disrupts its periodicity. One of the defects often used in practice is inversion, which consists of changing the order of layers in one of the two parts of the structure [23–25]. If a defect occurs in a structure at the boundary of adjacent periods, then the transfer matrix of the structure in this case has the form $\hat{S} = (\hat{M})^m(\tilde{\hat{M}})^m$, where the transfer matrix $\hat{M} = \hat{N}_1 \cdot \hat{N}_2$ corresponds to the original period, and the matrix $\tilde{\hat{M}} = \hat{N}_2 \cdot \hat{N}_1$ corresponds to the inverted period. The matrix elements of the transfer matrix of the inverted period are related to the elements of the matrix of the normal period by the relation $(\tilde{\hat{M}})_{\alpha\beta} = (\hat{M})_{3-\beta,3-\alpha}$, where $\alpha, \beta = 1, 2$. The presence of such a defect leads to the appearance of a defect-free transmission miniband structure (defect mode) in the GB.

Figure 8 shows the frequency dependences of the coefficients R, T, A for the structures $(SiO_2/Si)^{10}(Si/SiO_2)^{10}$ and $((SiO_2/Gr)^{10}/Si)^{10}(Si/(SiO_2/Gr)^{10})^{10}$ with an inversion defect (a) in the case of quarter-wave thicknesses of layers L_1, L_2, and the values of the chemical potential of graphene $\mu = (0.2,\ 0.4,\ 0.8\,\text{eV}$ (b, c, d, respectively). The presence of a defect in a structure without graphene layers leads to the appearance in the center of the PBG of a defect-free structure of an allowed miniband, in the center of which the reflectance decreases to almost zero, and the transmission factor can be close to unity (see inset on the right). In a structure with graphene outside the PBG, the frequency dependence of the optical factors is close to the corresponding dependences for a defect-free structure (Fig. 6). Inside the PBG, a significant restructuring of the indicated dependencies occurs, as demonstrated by the curves shown on an enlarged scale (to the right of the general figure) for the first PBG. It can be seen that in the structure with graphene at $\mu = 0.2\,$eV, the defect mode is suppressed in the first PBG (as a result of which transmission is completely absent). With an increase in the chemical potential, the defect mode is restored, but for this mode there is not only reflection, but also transmission with absorption. As the chemical potential increases, the defect mode shifts to higher frequencies. In the second PBG at all values of μ there is no transmission, and reflection exceeds absorption, while the dependence on the chemical potential is practically absent.

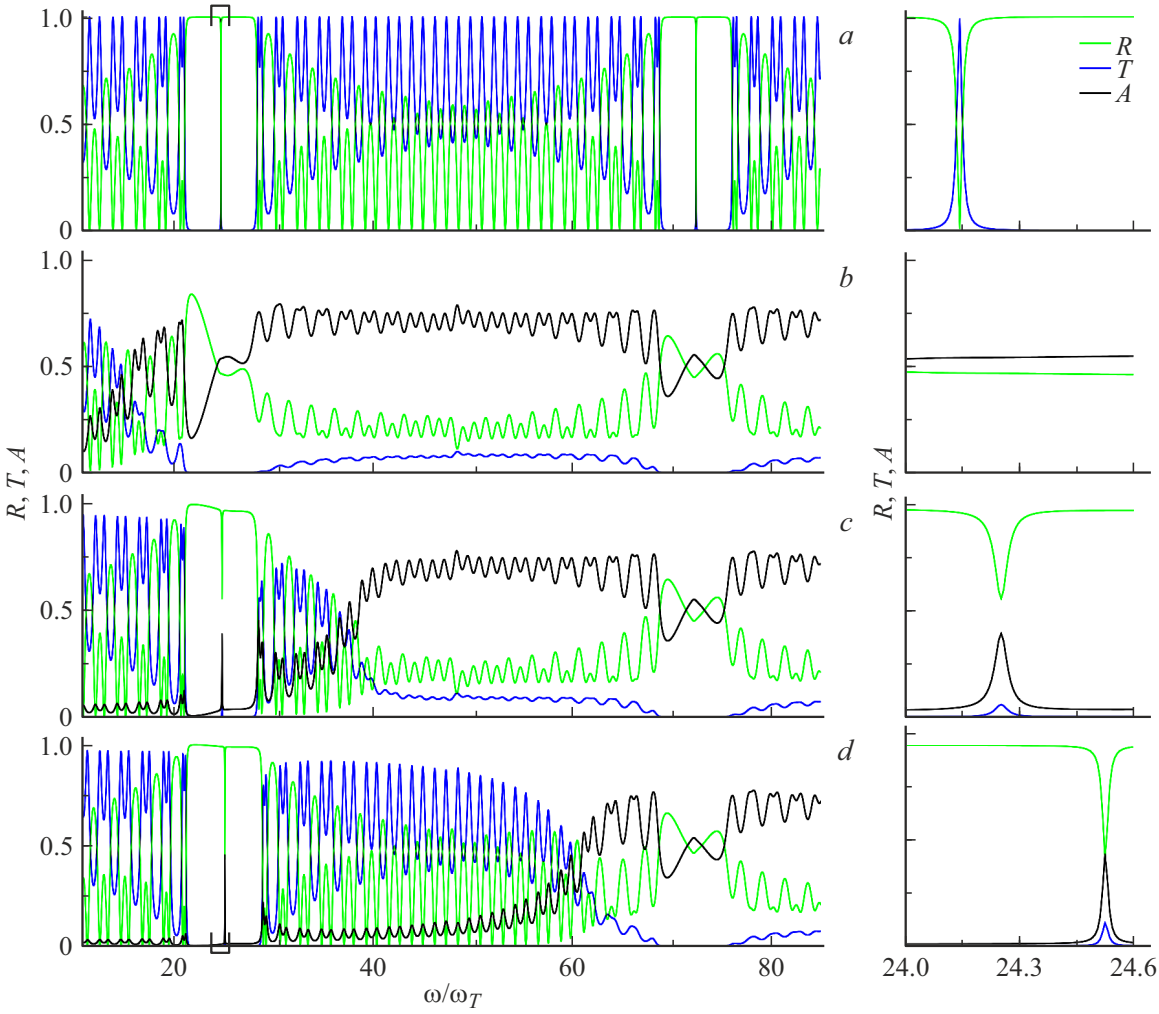

Figure 8. Frequency dependence of the factors R, T and A for the structures $((SiO_2)^{10}/Si)^{10}(Si/(SiO_2)^{10})^{10}$ (a) and $((SiO_2/Gr)^{10}/Si)^{10}(Si/(SiO_2/Gr)^{10})^{10}$ with $\mu = (0.2, 0.5, 0.8)$ eV (b, c and d respectively).

Conclusion

The presence of graphene layers in PCS leads to a significant dependence of the nature of the spectra on the chemical potential of graphene. Changing the chemical potential allows to rearrange photon spectra, changing over a wide range the reflection, transmission and absorption of radiation incident on the structure. In particular, areas appear in the spectra in which transmission is completely absent, reflection is relatively small, and the maximum part of the incident radiation is absorbed. The diagrams in the corresponding frequency intervals contain both regions of total reflection and areas of complete absorption of radiation, which allows the use of PCS as an effective reflector or absorber of radiation.

The presence of an inversion defect leads to the appearance in the reflection and transmittance spectra of a non-absorbing PCS of one transmission miniband in the photonic BG of a defect-free crystal. The presence of graphene leads to the presence of absorption in the spectrum and partial or complete suppression of the defect mode, as well as transmission in general. The formation of a PCS based on an effective graphene medium allows not only to control the photon spectrum and the width of the PGB by changing the structure parameters, number of periods, and chemical potential, but also to use it as a spectrally sensitive filter or radiation absorber.

Funding

This study was supported financially by the Ministry of Science and Higher Education of the Russian Federation under State Assignment FEUF-2023-0003.

Conflict of interest

The authors declare that they have no conflict of interest.

References

[1] S.V. Morozov, K.S. Novoselov, A.K. Geim. UFN, **178** (7), 776 (2008) (in Russian).
[2] A. Madani, S.R. Entezar. Phys. B, **431**, 1 (2013).
[3] M. Zamani, M. Abbasnejad. Physica C: Superconductivity and its Applications, **554**, 19 (2018).
[4] B. Kuzmenko, E. van Heumen, F. Carbone, D. van der Marel. Phys. Rev. Lett., **100** (11), 117401 (2008).
[5] R.R. Nair, P. Blake, A.N. Grigorenko, K.S. Novoselov, T.J. Booth, T. Stauber, N.M.R. Peres, A.K. Geim. Science, **320**, 1308 (2008).
[6] K.F. Mak, M.Y. Sfeir, Ya. Wu, C.H. Lui, J.A. Misewich, T.F. Heinz. Phys. Rev. Lett., **101**, 196405 (2008).
[7] Z. Ahmad, E.A. Muljarov, S.S. Oh. Phys. Rev. B, **104** (8), 085426 (2021).
[8] M.S.D. Vasconcelos, M.G. Cottam. J. Phys. D: Appl. Phys., **53** (13), 135101 (2020).
[9] M.A. Othman, C. Guclu, F. Capolino. Opt. Express, **21** (6), 7614 (2013).
[10] D. Jahani, A. Soltani-Vala, J. Barvestani, H. Hajian J. Appl. Phys., **115**, 153101 (2014).
[11] S.A. El-Naggar Opt. Quant. Electron., **47** (7), 1627 (2015).
[12] S. Razi, F. Sepahi, A.A. Saray. Physica B: Condensed Matter, **597**, 412380 (2020).
[13] X.H. Deng, J.T. Liu, J.R. Yuan, Q.H. Liao, N.H. Liu. Europhys. Lett., **109**, 27002 (2015).
[14] L.A. Falkovsky J. Phys.: Conference Series, **129** (1), 012004 (2008).
[15] T. Zhang, M.Y. Mao, Y. Ma, D. Zhang, H.F. Zhang. Optik, **223**, 165636 (2020).
[16] D.A. Smirnova, I.V. Iorsh, I.V. Shadrivov, Y.S. Kivshar. JETP Lett., **99** (8), 456 (2014).
[17] A. Rashidi, A. Namdar, R. Abdi-Ghaleh. Superlattices and Microstructures, **105**, 74 (2017).
[18] A. Madani, S.R. Entezar. Superlattices and Microstructures., **86**, 105 (2015).
[19] K.I. Bolotin, K.J. Sikes, Z. Jiang, M. Klima, G. Fudenberg, J. Hone, P. Kim, H.L. Stormer. Sol. Stat. Commun., **146** (9–10), 351 (2008).
[20] V. Ryzhii, A. Satou, T. Otsuji. J. Appl. Phys., **101** (2), 024509 (2007).
[21] C. Attaccalite, L. Wirtz, M. Lazzeri, F. Mauri, A. Rubio. Nano Lett., **10**, 1172 (2010).
[22] M. Born, E. Wolf. Principles of Optics: Electromagnetic Theory of Propagation, Interference and Diffraction of Light (Elsevier, 2013).
[23] J. Fu, W. Chen, B. Lv. Phys. Lett. A, **380** (20), 1793 (2016).
[24] W. Belhadj, N.B. Ali, H. Dakhlaoui, O.H. Alsalmi, H. Alsaif, A. Torchani. The Eur. Phys. J. B, **94** (10), 1 (2021).
[25] H. Da, G. Liang. Appl. Phys. Lett., **98** (26), 261915 (2011).

Translated by E.Potapova